Journal of Applied Polymer Science

Phase appearance during polymerization of fluorinated polyimide monomers and deposition into the microscopic-scale trenches in supercritical carbon dioxide

Masashi Haruki, Asuka Oda, Atsuhiko Wasada, Yumi Hasegawa, Shin-ichi Kihara, Shigeki Takishima
Department of Chemical Engineering, Graduate School of Engineering, Hiroshima University, 1-4-1 Kagamiyama, Higashi-Hiroshima 739-8527, Japan
Correspondence to: M. Haruki (E-mail: mharuki@hiroshima-u.ac.jp)

ABSTRACT: The phase appearance during the synthesis of fluorinated polyamic acid (PAA) from 2,2-bis(3,4-anhydrodicarboxyphenyl)-hexafluoropropane (6FDA) and 2,2′-bis(trifluoromethyl)−4,4′-diaminobiphenyl (TFDB) in supercritical carbon dioxide ($scCO_2$) was investigated to obtain fundamental data for the deposition of fluorinate polyimides (PI) using $scCO_2$. All polymerizations were carried out at 30 MPa for 60 min. The experimental temperatures ranged from 50 to 70 °C, and each of the monomer concentrations ranged from 0.67×10^{-5} to 3.3×10^{-5} mol cm^{-3}. The holding time of the transparent phases, which was the time from the beginning of the polymerization to the appearance of a turbid phase, was increased with either a decrease in the polymerization temperature or a decrease in the initial monomer concentration. The holding time of the fluorinated PAA was longer than that of the monomers of Kapton-type PAA. The deposition of PI into the microscopic-scale trenches that had formed on the silicon wafer was successful in $scCO_2$. © 2016 Wiley Periodicals, Inc. J. Appl. Polym. Sci. **2016**, *133*, 43334.

KEYWORDS: films; polyimides; synthesis and processing

Received 12 August 2015; accepted 14 December 2015
DOI: 10.1002/app.43334

INTRODUCTION

Polyimide (PI) is widely used for engineering plastics because it has excellent mechanical strength and heat resistance by comparison with other polymers. Moreover, PI is also known as an excellent electrical insulation material due to a quite low dielectric constant.[1–3] It is well known that the dielectric constant, refraction index, and water absorbability can be reduced via the introduction of fluorinated groups into the chemical structure of PI, although the addition of fluorinated groups leads to decreases in the chemical resistance, glass transition temperature, and affinity for other materials.[4,5] Therefore, fluorinated PI has been applied as a polarization element and an optical waveguide in optical devices.[6,7]

PI is commonly produced from a tetracarboxylic dianhydride and a diamine via the polyamic acid (PAA) of an intermediate, as shown in Figure 1. Among many fluorinated PI monomers, 2,2-bis(3,4-anhydrodicarboxyphenyl)-hexafluoropropane (6FDA) is often used as a tetracarboxylic dianhydride. On the other hand, a wide variety of diamines have been used for the production of fluorinated PIs. Matsuura *et al.* researched the solubility of PIs constructed by 6FDA and 2,2′-bis(trifluoromethyl)-4,4′-diaminobiphenyl (TFDB), which were imidized at different temperatures in eight types of organic solvents. The PI of 6FDA - TFDB, even when imidized at 350 °C, dissolved easily in *N*,*N*-dimethyl acetamide, acetone, tetrahydrofuran, and ethyl acetate. Moreover, PI cured at 200 °C could be dissolved even in chloroform and methanol, although this was not easy. Furthermore, the values for coefficient of thermal expansion (CTE) were also discussed for the fluorinated PI of 6FDA–TFDB and for copolyimides that included 6FDA–TFDB elements.[8,9] Moreover, Harris *et al.* focused on another TFDB-based fluorinated PI: 3,3′,4,4′-biphenyltetracarboxylic dianhydride (BPDA, not fluorinated tetracarboxylic dianhydride)—TFDB, and investigated its crystal structures and thermal stability.[10–13] The results of both research groups indicated that the CTE increased with increases in the fluorine content. This result indicated that the CTE can be adjusted in accordance with that of ground materials by controlling the fluorine content when the thin film layers are deposited.

Advanced functional devices consisting of PI have become smaller and more highly functionalized year by year, and the microscopic-scale processing of PI has become necessary. Vapor deposition polymerization (VDP) is often used to deposit a thin film on the surface

Additional Supporting Information may be found in the online version of this article.

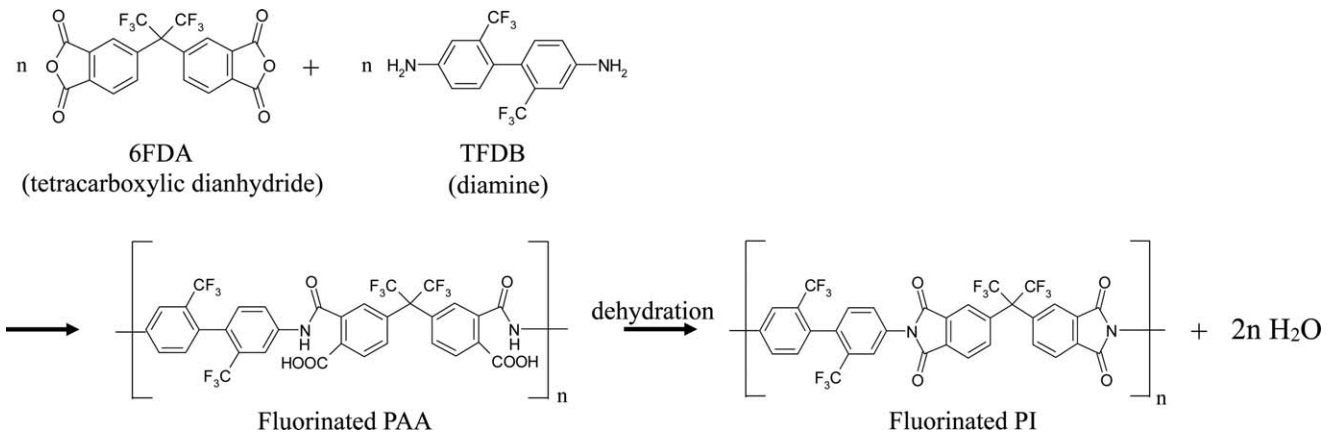

Figure 1. Reaction formula for the production of fluorinated PI from 6FDA and TFDB.

inside a microscopic-scale space. VDP is a dry process, which requires no solvent removal, and produces films with a uniform thickness.[14,15] As for the VDP of fluorinated PI, Maruo *et al.* investigated the deposition of fluorinated PI produced from 6FDA and TFDB on SiO_2/Si substrates.[16] They observed surface morphologies using several analytical instruments such as a scanning electron microscope (SEM) and an atomic force microscope (AFM) after the temperatures of the monomer sources were properly adjusted. The disadvantage of VDP is that the deposition rate is often low because the monomer supply rates strongly depend on the vapor or the sublimation pressures of monomers, although these are not usually high.[17–19]

Recently, we reported an alternative technique for the deposition of PI film inside a microscopic space using supercritical carbon dioxide ($scCO_2$). This allowed the deposition of PI films synthesized from PMDA and ODA of Kapton-type PI monomers onto the walls inside the trenches (width: 5 μm, depth 30 μm).[20] As for the deposition of PI from PMDA and ODA, they reacted immediately to produce PAA, although $scCO_2$ is a poor solvent for PAA. Therefore, deposition proceeded under some portions of the PAA had precipitated from the $scCO_2$ phase. These precipitated PAAs were discharged from the reactor or accumulated on the bottom of the reactor without contributing to the film formation. Moreover, the precipitated PI covered the outside surfaces of the microscopic pores, which blocked the monomers and low-molecular-weight PAAs from entering the microscopic spaces. To overcome this problem, a decrease in the reaction rate from monomers to PAA is considered effective, and the low reaction rate of the fluorinated PI monomers is interesting, as well as the optical and electrical properties of the fluorinated PI. The present study focused on a fluorinated PI consisting of 6FDA and TFDB, and the reaction from the monomers to the PAA was first investigated in $scCO_2$ to clarify the reaction behavior. Moreover, the deposition of fluorinated PI into microscopic-scale trenches using $scCO_2$ was also examined.

EXPERIMENTAL

Materials

Fluorinated PI monomers of 6FDA with purity >99 wt % and TFDB with purity >99.9 wt % were supplied by Daikin Industries. Both monomers were solid materials at room temperature, and the chemical structures are shown in the reaction scheme of Figure 1. CO_2 with purity >99.5 vol % was purchased from Chugoku Sanso. These materials were used without further purification. Moreover, *N*,*N*-dimethylformamide (DMF) with purity >99.7 vol %, which was used as a cosolvent added to $scCO_2$ and a moving bed for gel permeation chromatography (GPC), was purchased from Nacalai Tesque. Before use, the DMF was dehydrated using molecular sieves.

Apparatus and Procedure for Polymerization in $scCO_2$

An apparatus based on a static method equipped with CO_2 and monomer introduction portions was used to investigate the polymerization of 6FDA and TFDB in $scCO_2$ with 20 mol % of DMF, and the details of the apparatus and procedure can be found in a previous paper.[21] Therefore, only the procedure of the experiment is briefly described here. First, a high-pressure cell (Toyo Koatsu, an internal diameter of 10 mm and an internal volume of 17.1 cm^3) equipped with Pyrex windows for visual observation was heated to the experimental temperature using cartridge heaters. A certain amount of the DMF + TFDB solution, for which the concentration of TFDB had been previously determined, was then introduced into the cell. Pure CO_2 was introduced using an HPLC pump (Jasco, PU-2080-CO_2 Plus), and the amount of CO_2 in the cell was estimated by the pressure, temperature, cell volume, and volume of mixing data for the CO_2 + DMF system.[22] Finally, 6FDA dissolved in DMF was added to the cell using another HPLC pump (Jasco, PU-2080 Plus) in such a way that the molar quantity of 6FDA was equal to that of the TFDB while the pressure inside the cell was raised to about 30 MPa, and the polymerization reaction to PAA was initiated. The phase appearance inside the cell was observed using a borescope (Olympus, R100 series) with a CCD camera (Sanyo, VCC D473) system through the Pyrex windows. After the polymerization was finished, PAA that had dissolved in DMF was collected. The molecular weights of PAA were determined via the GPC system, and were calibrated using standard monodisperse polyethylene glycols and polyethylene oxides. The details of the GPC analysis method, including information concerning the columns that were used, are described in a previous paper.[21]

Apparatus and Procedure for Deposition into Microscopic-scale Trenches in $scCO_2$

An apparatus for the deposition of PI was developed in a previous study.[23] This apparatus was based on the flow method, which consists

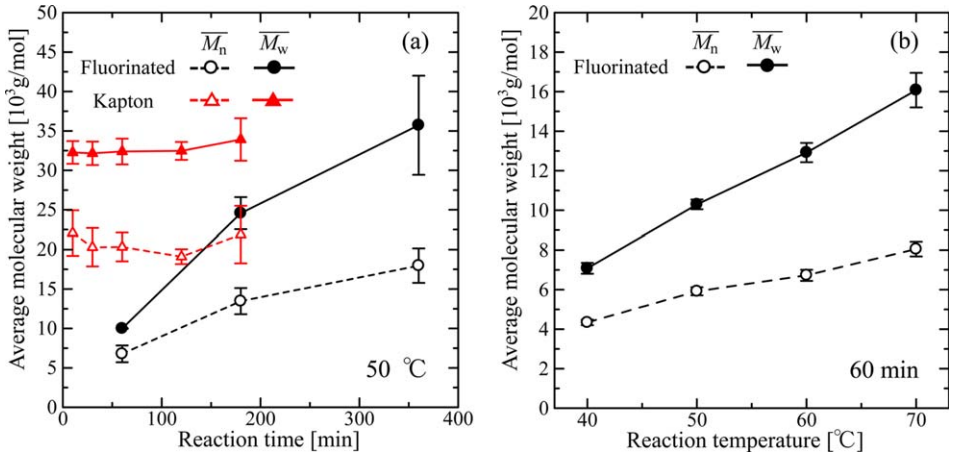

Figure 2. Relationships between the experimental conditions and the average molecular weights for polymerization of 6FDA and TFDB in pure DMF at each initial monomer concentration of 6.5×10^{-5} mol cm^{-3}. (a): Relationships of the reaction time and average molecular weight at 50 °C along with that for Kapton-type PAA polymerized at each initial monomer concentration of 6.6×10^{-5} mol cm^{-3} and at 10 °C; (b): Temperature dependency of the average molecular weights of the 6FDA–TFDB type PAA for the reaction time of 60 min. [Color figure can be viewed in the online issue, which is available at wileyonlinelibrary.com.]

of two supply lines for each monomer dissolved in $scCO_2$ with DMF as a cosolvent and a cold-wall-type deposition reactor (Toyo Koatsu, 100 mL of internal volume) located in a thermostatic air bath. Details of the apparatus are described in the previous paper mentioned above, and an outline of the deposition procedure is shown here.

A silicon wafer with either lattice- or line-shaped trenches was set on an aluminum stage covered by a heat insulator made of polyimide blocks. The silicon wafer was 10 mm × 10 mm in size, and the trenches were 5-μm wide and 30-μm deep for both shapes of trenches. In the reactor, the wafer was fixed on the ceiling position, and monomers were supplied from underneath. The supply ports for each of the monomers were in close proximity in the cell, and the distance between the ports and the substrate was about 5 mm. In the present work, depositions were carried out at 200 or 250 °C of the aluminum stage temperature and at 30 MPa for 90 min. Each monomer was supplied into the reactor at a concentration of 1.1×10^{-5} mol cm^{-3} after being heated at 50 °C in the thermostatic air bath. Following deposition, pure $scCO_2$ was introduced into the reactor to remove DMF from inside the reactor with the values for substrate temperature, reactor temperature, and pressure all maintained as those during deposition.

The morphologies of the PIs deposited onto the substrates were investigated using an SEM (Hitachi High-Technologies, S-5200) equipped with an energy-dispersive X-ray spectrometer (EDX, Edax, Genesis XM2). Moreover, the chemical structure of the deposited PI was analyzed using a Fourier transform infrared (FT-IR) spectrometer (Thermo Scientific, Nicolet is5) based on the ATR method.

RESULTS AND DISCUSSION

Relationships between Polymerization Time and Temperature, and the Molecular Weight of PAA in Pure DMF

Before the investigations of the polymerization in $scCO_2$, the relationships between the polymerization time and temperature, and the molecular weight of the synthesized PAA were studied in pure DMF to obtain fundamental perceptions. The reactivity of a tetracarboxylic dianhydride increases as the electron density at the carbonyl group decreases, and the reactivity of diamine increases with increasing electron density at the nitrogen atom in the amino group.[24] Therefore, the polymerization rate of 6FDA and TFDB had been expected to be lower than that of the Kapton-type monomers of PMDA and ODA.

The relationships between the polymerization time, and the number and weight average molecular weights ($\overline{M_n}$ and $\overline{M_w}$) of PAA are shown in Figure 2. The polymerizations were carried out using 6.5×10^{-5} mol cm^{-3} of each of the monomer concentrations at a temperature of 50 °C. As shown in the figure, both the $\overline{M_n}$ and $\overline{M_w}$ of PAA was increased significantly up to 360 min. These results indicated that the polymerization still proceeded well at least up to 180 min at 50 °C. The results of the polymerization of PMDA and ODA of Kapton-type PI monomers at 6.6×10^{-5} mol cm^{-3} and at 10 °C are also shown in the figure as a reference. A comparison of the results for the fluorinated monomers with that of the Kapton-type monomers indicated that the reaction rate of the fluorinated monomers was much lower than that of the Kapton-type monomers in pure DMF, although the reaction temperature of the fluorinated monomers was 40 °C higher than that of the Kapton type. These results corresponded well with the explanations shown in the literature,[24] as previously described.

Moreover, the polymerization temperature dependencies for both the $\overline{M_n}$ and $\overline{M_w}$ of PAA are also described in Figure 2. All polymerizations were carried out for 60 min, and both the $\overline{M_n}$ and $\overline{M_w}$ increased from 4.3×10^3 to 8.1×10^3 and from 7.1×10^3 to 1.6×10^4 g mol^{-1}, respectively, in an approximately linear fashion as the temperature was increased from 40 to 70 °C. Based on the obtained relationships between the polymerization time and the molecular weights, these temperature dependencies of the $\overline{M_n}$ and $\overline{M_w}$ were considered to have been due to an increase in the reaction rate as the temperature was increased rather than to a temperature dependency of the reaction equilibrium.

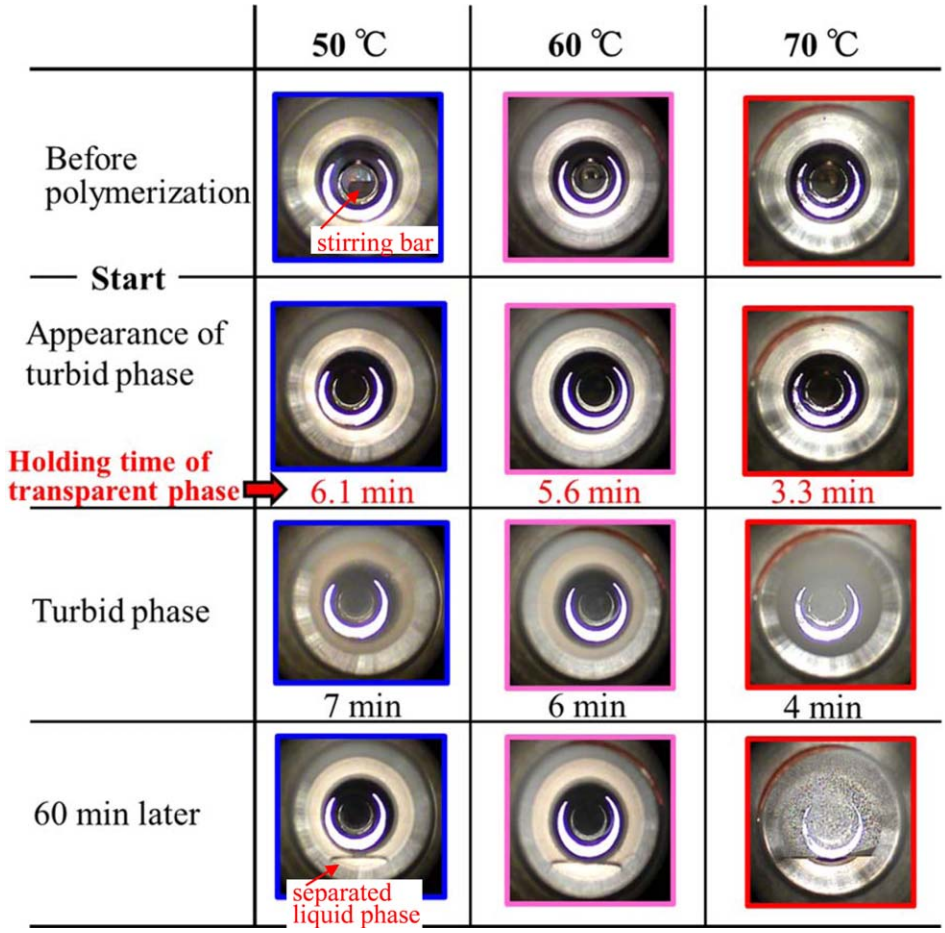

Figure 3. Chronological changes in the phase behaviors during the polymerization of 6FDA and TFDB in $scCO_2$ with 20 mol % of DMF at 30 MPa and at each monomer concentration of 2.0×10^{-5} mol cm^{-3}. [Color figure can be viewed in the online issue, which is available at wileyonlinelibrary.com.]

Phase Appearance and Molecular Weight of PAA Polymerized in $scCO_2$

The polymerizations were carried out in $scCO_2$ with 20 mol % of DMF for each of 6FDA and TFDB concentrations ranging from 6.7×10^{-6} to 3.3×10^{-5} mol cm^{-3} at temperatures ranging from 50 to 70 °C, and at polymerization times of 60 min. The images of the phase appearance in the high-pressure cell during polymerization at temperatures from 50 to 70 °C and at concentrations of 2.0×10^{-5} mol cm^{-3} for both monomers are shown in Figure 3. The transparent phase of the TFDB + DMF + $scCO_2$ solution was observed, and the stirring bar could be identified before the addition of the 6FDA + DMF solution into the cell at all reaction temperatures. After polymerization was initiated by the addition of 6FDA, the transparent phase was maintained for a certain time before changing into a turbid phase. The duration of the transparent phase depended on the temperature. With a further progression of polymerization, the liquid phase that was separated from the $scCO_2$ phase gradually accumulated at the bottom of the cell.

The relationships between the experimental conditions and the holding time of the transparent phase are shown in Figure 4 along with the results obtained from the polymerization of PMDA and ODA at each monomer concentration of 1.2×10^{-5} mol cm^{-3} and at a temperature of 50 °C. The transparent phase during the reaction of 6FDA and TFDB could be maintained much longer than that of the polymerization of PMDA and ODA, although the monomer concentrations of PMDA and ODA were much lower. The low polymerization rate of fluorinated PI monomers is expected to become an advantage for the deposition of PI inside the microscopic spaces using $scCO_2$ because many monomers can be delivered before they react to high-molecular-weight PAA that is insoluble in $scCO_2$.

Moreover, as the temperature decreased from 70 to 50 °C, the holding time increased from about 3 to 6 min at each monomer concentration of 2.0×10^{-5} mol cm^{-3}. As for each monomer concentration of 3.3×10^{-5} mol cm^{-3}, the same temperature dependency as that of 2.0×10^{-5} mol cm^{-3} was observed for the holding time of the transparent phase. These temperature dependencies on the holding time are considered to be due to change in the reaction rates based on differences in the temperatures. Namely, the rate of molecular weight (polymerization degree) increase with increases in temperature was the same manner as the polymerization in pure DMF shown in Figure 2. As for the monomer concentration effect, the holding times decreased with increases in the initial monomer concentration of between 0.67×10^{-5} and 3.3×10^{-5} mol cm^{-3}.

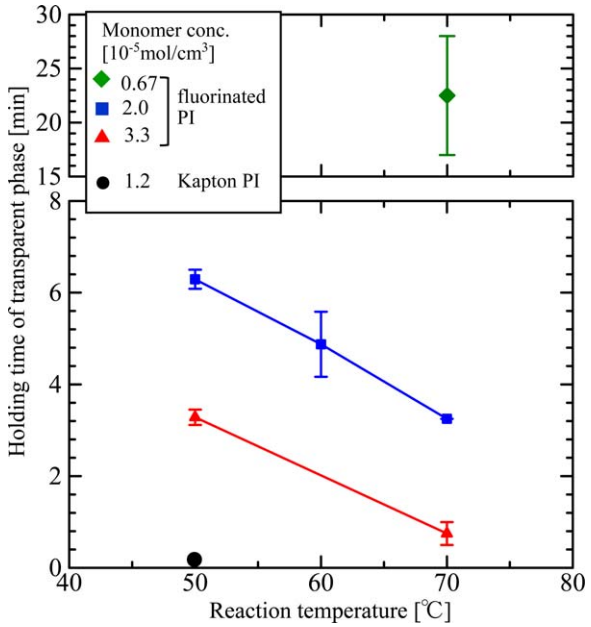

Figure 4. Effect of reaction temperature and initial monomer concentrations on the holding time of the transparent phase for the polymerization of 6FDA and TFDB in $scCO_2$ with 20 mol % of DMF at 30 MPa for 60 min. [Color figure can be viewed in the online issue, which is available at wileyonlinelibrary.com.]

The $\overline{M_w}$ of the PAAs obtained under each polymerization condition for 60 min are shown in Supporting Information Figure S1 of the Supporting information as reference data. As shown in Figure 3, a phase separation occurred during polymerization and a liquid polymer-rich phase accumulated at the bottom of the reactor as the polymerization progressed. Therefore, the data should be taken into consideration the fact that the precipitated PAA was condensed in the liquid phase and that the polymerization would have accelerated there. The $\overline{M_w}$ was increased with increases in both temperature and the initial monomer concentrations as shown in the figure. These results corresponded to trends in the holding times of the transparent phase, although polymerization progressed in both the CO_2 and liquid phases.

Deposition of the Fluorinated PI into the Microscopic-scale Trenches

The cross-section SEM images of the outer surfaces and the inside of the wafers with lattice-shaped trenches are shown in Figure 5. The operating conditions of the depositions were as follows: 200 °C for substrate temperature, 30 MPa and 90 min for deposition pressure and duration, respectively, and 1.1×10^{-5} mol cm^{-3} for each feed monomer concentration under conditions of 50 °C and 30 MPa for the feed lines in the thermostatic air bath, as previously described. Also, 10 mol % of DMF was added as a cosolvent. As shown in Figure 5, the fluorinated PI films covered the outer surface of the trenches. Furthermore, the trenches were completely filled with the fluorinated PI from bottom to surface, although only the thin film could be deposited in the same size trenches used in the present work for the Kapton-type PI. The results of the EDX analyses indicated that the PI was embedded in the trenches. On the other hand, small amounts of interspaces that were observed between the PI and Si walls may have been caused by a volumetric shrinkage based either on differences in deposition and atmospheric temperature or on the removal of CO_2 and DMF dissolved in PI and PAA. Moreover, the cross-section SEM images of the Si wafer with line-shaped trenches after the deposition of PI are shown in Figure 6. In this case, 5 mol% of DMF was added to $scCO_2$ as a cosolvent. The 5 μm (width) $\times$ 30 μm (depth) line-shaped trenches were formed at 45-μm intervals. The PI was deposited on the outer surface of the Si wafer, and the thickness of the film depended on the position. Cross-sectional SEM analyses were carried out for wide ranges of the "analytical cross-sections 1 and 2," as indicated in the figure. As shown in the SEM image and the results of the EDX analyses, the PI was firmly embedded in the trenches from the bottom to top positions. We checked 119 trenches of the "analytical cross-sections 1 and 2," as shown in Figure 6(b), and for 99% of the trenches, the PI was fully embedded, as shown by the results in Figure 6(c).

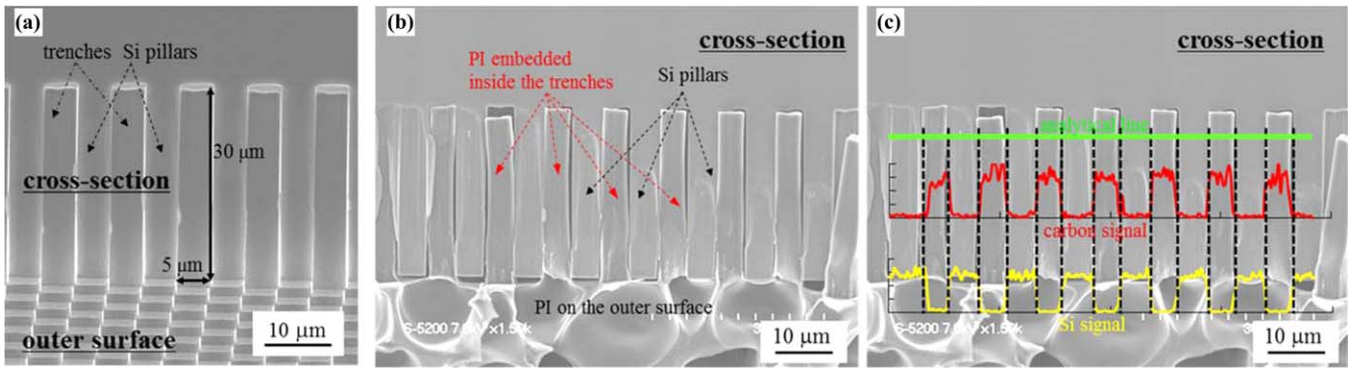

Figure 5. SEM images and the results of the EDX line analyses of the fluorinated PI deposited on the lattice-shaped trenches of an Si wafer at 200 °C and 30 MPa, and with DMF of 10 mol % for 90 min. (a): The SEM image of the Si wafer viewed from a tilted angle before deposition; (b): Cross-section SEM image of the Si wafer after the deposition; and, (c): The results of the EDX line analyses of the SEM image of (b) for carbon and Si atoms. [Color figure can be viewed in the online issue, which is available at wileyonlinelibrary.com.]

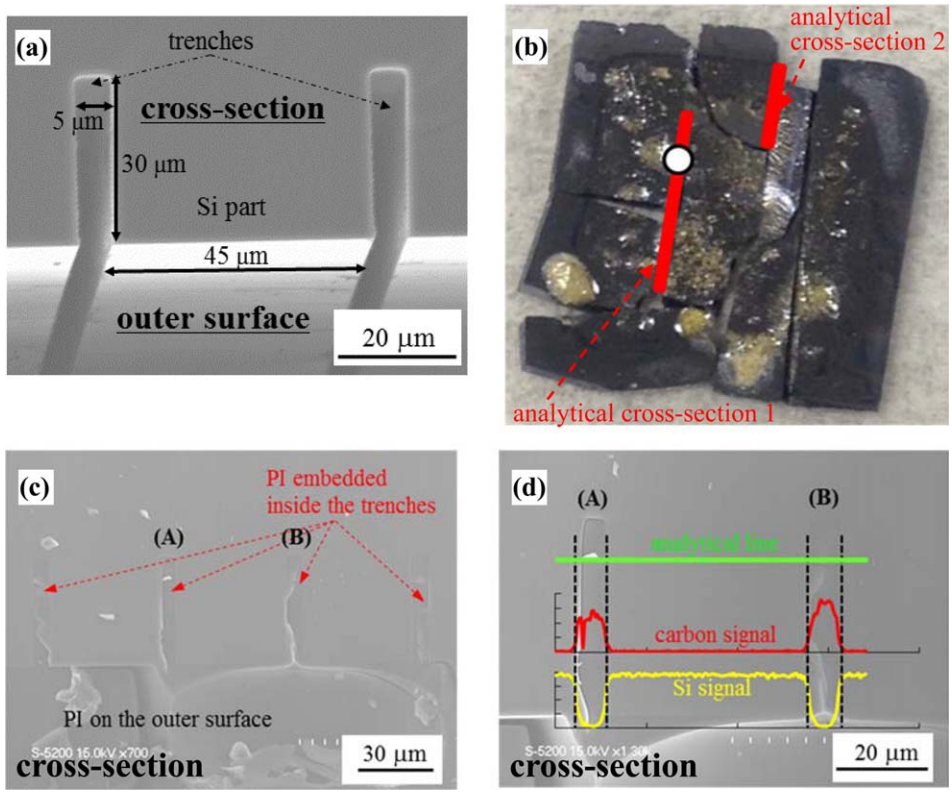

Figure 6. Images and the results of the EDX line analyses of the fluorinated PI deposited on the line-shaped trenches of an Si wafer at 250 °C and 30 MPa, and with DMF of 5 mol % for 90 min. (a): The SEM image of the Si wafer viewed from a tilted angle before deposition; (b): Surface image of the Si wafer after deposition obtained by a digital camera and indications of the SEM analytical positions; (c): Cross-section SEM image at the position indicated as the white circle in the image of (b); and, (d): The results of the EDX line analyses around the trenches of (A) and (B) in the SEM image of (c). [Color figure can be viewed in the online issue, which is available at wileyonlinelibrary.com.]

As described in our previous paper,[20] only the thin film of the Kapton type PI could be deposited in the same sized trenches used in the present work. However, we could not achieve a complete fill of the trenches with PI. One of the reasons for the difference in the deposition behavior between the fluorinated and Kapton-type PIs was thought to be the reaction rate for the polymerization of 6FDA and TFDB, which was much lower than that for PMDA and ODA. Therefore, greater amounts of unreacted and low molecular weight PI (6FDA and TFDB) were supplied into the trenches compared with the Kapton-type monomers. Moreover, a decrease in the polymerization rate in the bulk $scCO_2$ phase also led to a decrease in the sedimentation of the PI that reacted in the bulk $scCO_2$ phase with the outer surface of the trenches. Another possible reason for the difference in the deposition behaviors may be based on the difference in the solubilities of PAA and PI in the $scCO_2$ + DMF mixture. As described in the Introduction section, unlike Kapton-type PI, the PI that is formed by 6FDA and TFDB can dissolve in solvents. Therefore, the solubilities in the $scCO_2$ + DMF mixture would be different, and high solubility would prevent entrance into the trenches from being blocked by PI and PAA. Clarification of the differences in the deposition mechanisms based on the differences in the monomer species will be carried out in our future work.

The chemical structures of the deposited films were analyzed via FT-IR spectrometry along with the PAA and PI using 6FDA and TFDB as references. In the preparation, a sample of the deposited film was obtained via deposition onto the lattice-shaped trenches under the same conditions shown in Figure 5, and it was scratched off the outer surface of the wafer. On the other hand, a PAA reference sample was prepared by removing the DMF from the PAA solution obtained after polymerization in $scCO_2$ with 20 mol % of DMF at each monomer concentration of 3.3×10^{-5} mol cm^{-3} at 50 °C and 30 MPa. The reference PI samples were also prepared by the imidization of the same PAA solution by using a thermogravimetric analyzer, and the temperature was increased by 5 °C min^{-1} from room temperature to 350 °C, and then it was maintained at 350 °C for 60 min under a nitrogen atmosphere. The FT-IR spectra of these are described in Figure 7. The vibrational modes that were focused on were the C=O stretching found at 1540 and 1650 cm^{-1} for PAA,[25,26] as well as the C—N stretching, C=O symmetric stretching, and C=O asymmetric stretching at 1360, 1730, and 1790 cm^{-1}, respectively, for PI.[8,25–28] The figure shows that the spectrum of the deposited film was similar to the reference PI. Namely, recognizable peaks assigned to the vibrations of the chemical structures characterized as PAA could not be found, but the peaks representing the vibration modes of PI were observed. According to a NMR study into the imidization temperatures of 6FDA and TFDB-type PI by

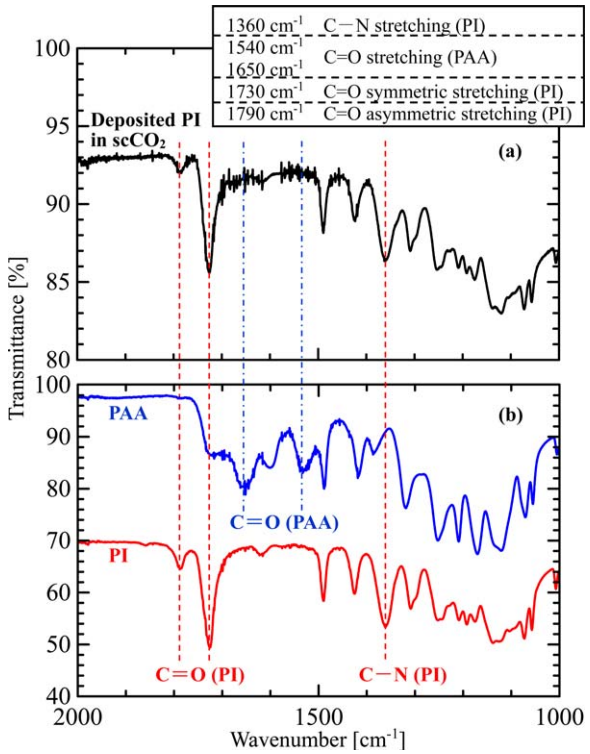

Figure 7. FT-IR spectra of the fluorinated PI deposited onto an Si wafer with lattice-shaped trenches at 200 °C and 30 MPa in $scCO_2$ with 10 mol % DMF for 90 min. (a): The spectrum of the fluorinated PI deposited in $scCO_2$; and, (b): The spectra of the fluorinated PAA and PI as references. [Color figure can be viewed in the online issue, which is available at wileyonlinelibrary.com.]

Matsuura et al.,[8] the imidization finishes at about 200 °C in dimethyl sulfoxide. The imidization behavior of the deposition in $scCO_2$ obtained in the present work corresponded with the results obtained using organic solvents reported in the literature.

CONCLUSIONS

In the present work, the phase appearance during the polymerizations of 6FDA and TFDB to form fluorinated PAA in $scCO_2$ was investigated at temperatures ranging from 50 to 70 °C. The holding time of the transparent phase from the beginning of the polymerization for the fluorinated monomers was much longer than that of PMDA and ODA of the Kapton-type PI monomers. The holding times increased with decreasing polymerization temperature and monomer concentrations due to the reduction in the reaction rate. When the fluorinated PI was deposited into the microscopic-scale trenches formed on the silicon wafers, the trenches were completely filled in both the lattice-shaped and line-shaped trenches. Moreover, the chemical structures of the deposited PI were analyzed via FT-IR spectrometry, and significant peaks indicating the existence of imide structures were observed. The peaks of PAA structures, however, could not be found for the deposited PI.

ACKNOWLEDGMENTS

This work was financially supported by JSPS KAKENHI Grant Numbers 23760722 and 26420765. The authors also thank the Research Institute for Nanodevice and Bio Systems of Hiroshima University, and the Nanotechnology Platform of the Ministry of Education, Culture, Science and Technology of Japan for the preparation of the silicon wafers with microscopic patterned trenches. They also thank Dr. Maeda, the Natural Science Center for Basic Research and Development (N-BARD), Hiroshima University, for much useful advice concerning film characterization using SEM with EDX.

REFERENCES

1. Kaneshiro, H.; Akahori, K. In Latest Polyimide; Yokota, R., Ed.; NTS Co.: Tokyo, **2010**; p 315 (in Japanese).
2. Lee, B. J.; Kim, H. G.; Lee, D. C. *Surf. Coat. Technol.* **2002**, *150*, 182.
3. Iwata, M.; Imagawa, K. In Latest Polyimide; Yokota, R., Ed.; NTS Co.: Tokyo, **2010**; p 417 (in Japanese).
4. Hougham, G. In Fluoropolymers 2, Properties; Hougham, G., Cassidy, P. E., Johns, K., Davidson, T., Eds.; Kluwer Academic: New York, **1999**; p 233.
5. Ando, S. In Latest Polyimide; Yokota, R., Ed.; NTS Co.: Tokyo, **2010**; p 102 (in Japanese).
6. Ma, H.; Jen, A. K. Y.; Dalton, L. R. *Adv. Mater.* **2002**, *14*, 1339.
7. Ando, S. *J. Photopolym. Sci. Technol.* **2004**, *17*, 219.
8. Matsuura, T.; Hasuda, Y.; Nishi, S.; Yamada, N. *Macromolecules* **1991**, *24*, 5001.
9. Matsuura, T.; Yamada, N.; Nishi, S.; Hasuda, Y. *Macromolecules* **1993**, *26*, 419.
10. Cheng, S. Z. D.; Arnold, F. E., Jr.; Zhang, A.; Hsu, S. L. C.; Harris, F. W. *Macromolecules* **1991**, *24*, 5856.
11. Cheng, S. Z. D.; Wu, Z.; Eashoo, M.; Hsu, S. L. C.; Harris, F. W. *Polymer* **1991**, *32*, 1803.
12. Eashoo, M.; Shen, D.; Wu, Z.; Lee, C. J.; Harris, F. W.; Cheng, S. Z. D. *Polymer* **1993**, *34*, 3209.
13. Arnold, F. E., Jr.; Cheng, S. Z. D.; Hsu, S. L. C.; Lee, C. J.; Harris, F. W. *Polymer* **1992**, *33*, 5179.
14. Takahashi, Y.; Iijima, M.; Inagawa, K.; Itoh, A. *J. Vac. Sci. Technol. A* **1987**, *5*, 2253.
15. Salem, J. R.; Sequeda, F. O.; Duran, J.; Lee, W. Y.; Yang, R. M. *J. Vac. Sci. Technol. A* **1986**, *4*, 369.
16. Maruo, Y. Y.; Andoh, Y.; Sasaki, S. *J. Vac. Sci. Technol. A* **1993**, *11*, 2590.
17. Takahashi, Y.; Matsuzaki, K.; Iijima, M.; Fukada, E.; Tsukahara, S.; Murakami, Y.; Maesono, A. *Jpn. J. Appl. Phys.* **1993**, *32*, L875.
18. Dutt, R.; Takahashi, Y.; Iijima, M. *Jpn. J. Appl. Phys.* **1999**, *38*, L687.
19. Papastrat, A. G.; Chu, T.; Anthamatten, M. *Chem. Vapor Deps.* **2011**, *17*, 141.
20. Haruki, M.; Hasegawa, Y.; Kihara, S.; Takishima, S. *J. Supercrit. Fluids* **2015**, *100*, 52.
21. Haruki, M.; Hasegawa, Y.; Fukui, N.; Kihara, S.; Takishima, S. *J. Appl. Polym. Sci.* **2014**, *131*, 39878.

22. Zúñiga-Moreno, A.; Galicia-Luna, L. A. *J. Chem. Eng. Data* **2005**, *50*, 1224.
23. Haruki, M.; Hasegawa, Y.; Fukui, N.; Kihara, S.; Takishima, S. *J. Supercrit. Fluids* **2014**, *94*, 147.
24. Morikawa, A.; Imai, Y. In Latest Polyimide; Yokota, R., Ed.; NTS Co.: Tokyo, **2010**; p 3 (in Japanese).
25. Hasegawa, M.; Kasamatsu, K.; Koseki, K. *Eur. Polym. J.* **2012**, *48*, 483.
26. Hasegawa, M.; Fujii, M.; Ishii, J.; Yamaguchi, S.; Takezawa, E.; Kagayama, T.; Ishikawa, A. *Polymer* **2014**, *55*, 4693.
27. Gao, H.; Yan, C.; Guan, S.; Jiang, Z. *Polymer* **2010**, *51*, 694.
28. Hasegawa, M.; Ishigami, T.; Ishii, J.; Sugiura, K.; Fujii, M. *Eur. Polym. J.* **2013**, *49*, 3657.